Classification of metal-oxide bonded interactions based on local potential- and kinetic-energy densities

G. V. Gibbs[a)]
Department of Geosciences, Materials Science, Engineering and Mathematics, Virginia Tech, Blacksburg, Virginia 24061

D. F. Cox
Department of Chemical Engineering, Virginia Tech, Blacksburg, Virginia 24061

T. D. Crawford
Department of Chemistry, Virginia Tech, Blacksburg, Virginia 24061

K. M. Rosso
W. R. Wiley Environmental Molecular Sciences Laboratory, Pacific Northwest National Laboratory, Richland, Washington 99352

N. L. Ross
Department of Geosciences, Virginia Tech, Blacksburg, Virginia 24061

R. T. Downs
Department of Geosciences, University of Arizona, Tucson, Arizona 85721

(Received 3 October 2005; accepted 1 December 2005; published online 24 February 2006)

A classification of the hydrogen fluoride H–F-bonded interactions comprising a large number of molecules has been proposed by Espinosa *et al.* [J. Chem. Phys. **117**, 5529 (2002)] based on the ratio $|V(\mathbf{r}_c)|/G(\mathbf{r}_c)$ where $|V(\mathbf{r}_c)|$ is the magnitude of the local potential-energy density and $G(\mathbf{r}_c)$ is the local kinetic-energy density, each evaluated at a bond critical point $\mathbf{r}_c$. A calculation of the ratio for the *M*–O bonded interactions comprising a relatively large number of oxide molecules and earth materials, together with the constraints imposed by the values of $\nabla^2\rho(\mathbf{r}_c)$ and the local electronic energy density, $H(\mathbf{r}_c)=G(\mathbf{r}_c)+V(\mathbf{r}_c)$, in the H–F study, yielded practically the same classification for the oxides. This is true despite the different trends that hold between the bond critical point and local energy density properties with the bond lengths displayed by the H–F and *M*–O bonded interactions. On the basis of the ratio, Li–O, Na–O, and Mg–O bonded interactions classify as closed-shell ionic bonds, Be–O, Al–O, Si–O, B–O, and P–O interactions classify as bonds of intermediate character with the covalent character increasing from Be–O to P–O. N–O interactions classify as shared covalent bonds. C–O and S–O bonded interactions classify as both intermediate and covalent bonded interactions. The C–O double- and triple-bonded interactions classify as intermediate-bonded interactions, each with a substantial component of covalent character and the C–O single-bonded interaction classifies as a covalent bond whereas their local electronic energy density values indicate that they are each covalent bonded interactions. The ratios for the Be–O, Al–O, and Si–O bonded interactions indicate that they have a substantial component of ionic character despite their classification as bonds of intermediate character. The trend between the ratio and the character of the bonded interactions is consistent with trends expected from electronegativity considerations. The ratio increases as the net charges and the coordination numbers for the atoms for several Ni-sulfides decrease. On the contrary, the ratio for the Si–O bonded interactions for the orthosilicate, forsterite, Mg_2SiO_4, and the high-pressure silica polymorph, stishovite, decreases as the observed net atomic charges and the coordination numbers of Si and O increase in value. The ratio for the Ni–Ni bonded interactions for the Ni-sulfides and bulk Ni metal indicate that the interactions are intermediate in character with a substantial component of ionic character. © *2006 American Institute of Physics*. [DOI: 10.1063/1.2161425]

INTRODUCTION

The properties of a solid-state material are governed by the crystal structure and by the types and the distribution of the bonded interactions.[1] Despite the fact that a chemical bond is not a quantum-mechanical observable, bonded interactions have been the central topic of numerous papers, review articles, and books devoted to the study and description of materials in terms of their chemical bonds.[2] In an important step towards advancing our understanding of the nature of the chemical bond, Pauling[3] forged his famous classification of bonded interactions based on electronegativity considerations as either ionic, covalent, or interactions of inter-

[a)]Electronic mail: gvgibbs@vt.edu

mediate bond type. Numerous other electronegativity scales have since been formulated, but a search of the chemical and physics literature reveals that Pauling's scale is one of the most frequently referenced in the study of bonded interactions.[4] As postulated, the greater the difference in the electronegativities for a pair of bonded atoms, the more ionic the asserted character of the interaction.[3] Consistent with this postulate, it is well known that binary MX materials consisting of bonded atoms M and X with large differences in their electronegativities tend to favor more densely packed ionic structures with either six or eight coordination numbers whereas those with smaller electronegativity differences tend to favor less dense more open covalent structures with four-coordinated atoms. As cation-anion radius ratio considerations often fail in the prediction of the coordination numbers for a material,[5] Mooser and Pearson[6] undertook a classification of the crystal structures for a large number of materials in terms of the electronegativity difference between the bonded atoms $\Delta\chi$ and the average principal quantum numbers of the valence electrons of the atoms $\tilde{n}$. Separation structure diagrams of $\Delta\chi$ versus $\tilde{n}$ for MX materials with the sphalerite, wurtzite, halite, and CsCl structure types show that the more covalent structures with four coordinate and the more ionic structures with six- and eight-coordinate M atoms appear in separate domains with little overlap. Additional separation diagrams for a relatively large number of MX_2, MX_3, M_2X_3, and M_2X materials also provided a subdivision of the structures with different coordination numbers into largely disjoint domains of structures with atoms with larger $\Delta\chi$ and $\tilde{n}$ values tending to be more dense, to possess larger coordination numbers and asserted to be more ionic.

In a widely cited study of the chemical bond and solid-state physics, Phillips[1] found that more than 80 materials with the diamond, zinc-blende, wurtzite, and rocksalt structures are separated uniquely into four- and six-coordinate disjoint domains when plotted against spectroscopically defined covalent and ionic energy gaps, C and E_h, respectively. Defining ionicity as $f_i = C^2/(E_h^2 + C^2)$, he found that the agreement between the f_i values with Pauling's[3] ionicities is "quite satisfactory, at least for qualitative purposes." More recently, structural separation plots have been generated for a very large number of materials in terms of the σ- and π-density-functional orbital radii of the bonded atoms.[7] With these radii, Zunger[7] was able to predict stable structures for more than 500 materials with remarkable success. As observed in earlier studies, he likewise found that the materials with the smaller radii tend to exhibit less dense structures with lower coordination numbers. In similar studies of pseudopotentials and crystal structures, Bloch and Schatteman,[8] among others, found that they could also reproduce Pauling's electronegativity scale reasonably well with a quantum-defect electronegativity scale, providing a further theoretical underpinning for the Pauling scale and strategy for estimating the character of bonded interactions. However, Pauling's strategy is not without its limitations. For example, values are defined for only a relatively few elements and it has yet to be used to gauge how the character of a given bonded interaction depends on the local structure as embodied in the variation of bond length, bond number, hybridization, coordination number, and the electron configuration of the bonded atoms.[4] In a study of hybridized orbitals, it was concluded, on the basis of a set of spectroscopically based electronegativities,[4] that the greater the s character of a bonded interaction, the greater the electronegativities of the bonded atoms, simply because s electrons have a lower energy than p electrons, resulting in the σ-orbital ordering rule (lowest to highest electronegativity) $sp^3 < sp^2 < sp$.

In addition to the advances made in the derivation and characterization of crystal structures using quantum-mechanical strategies and the classification of bonded interactions in terms of their thermochemical and spectroscopic properties, recent work[2,9] has shown that the bonded interactions of a material can be classified in terms of the bond critical point and local energy density properties of an electron-density distribution. In a theoretical modeling and characterization of the distributions for a wide variety of molecules, Bader and Essén[10] forged a quantitative strategy for classifying bonded interactions based on the local form of the virial equation $2G(\mathbf{r}_c) + V(\mathbf{r}_c) = (1/4)\nabla^2\rho(\mathbf{r}_c)$ where $G(\mathbf{r}_c)$ is the local kinetic-energy density, $V(\mathbf{r}_c)$ is the local potential-energy density, and $\nabla^2\rho(\mathbf{r}_c)$ is the Laplacian of the electron-density distribution $\rho(\mathbf{r}_c)$, each evaluated at the $(3, -1)$ critical points $\mathbf{r}_c$ of the interactions. The sign of $\nabla^2\rho(\mathbf{r}_c)$ is determined by the relative magnitudes of $G(\mathbf{r}_c)$ and $V(\mathbf{r}_c)$. When the magnitude $V(\mathbf{r}_c)$ is greater than $2G(\mathbf{r}_c)$, the Laplacian is necessarily negative, indicating that electron density is tightly bound and locally compressed above the average distribution at $\mathbf{r}_c$ along the bond path. In contrast, when the magnitude $V(\mathbf{r}_c)$ is less than $2G(\mathbf{r}_c)$, the Laplacian is necessarily positive, indicating that electron density is expanded relative to the average distribution and locally depleted at $\mathbf{r}_c$. On the basis of these results, a bonded interaction is classified as a shared covalent interaction when the Laplacian is negative and the value of the electron density at $\mathbf{r}_c$ is relatively large. On the other hand, when the Laplacian is positive and the value of the electron density is relatively small at $\mathbf{r}_c$, then the bonded interaction is classified as closed-shell ionic. The strategy was found to be successful, with a few exceptions,[2] in classifying the bonded interactions for a relatively wide variety of molecules, particularly for those involving first row atoms.[9] However, for second-row metal M atoms bonded to O, $\nabla^2\rho(\mathbf{r}_c)$ was found to be large and positive[11] (15–25 $e/\text{Å}^5$), indicating that selected Al–O, Si–O, P–O, and S–O bonds are, for example, closed-shell ionic interactions.

In an earlier study of the bond critical point and local energy density properties of the electron-density distributions for an additional set of molecules with first row atoms, optimized at the 6-31G* level, Cremer and Kraka[2] found that the Bader and Essén strategy[10] satisfactorily classifies the bonded interaction for the bulk of a number of the covalent- and ionic-bonded molecules. But they found that the Laplacian values for covalent double and triple CO bonds are positive (20.2 and 41.5 $e/\text{Å}^5$, respectively), a result that suggests that the condition that the Laplacian must be negative is not sufficient to classify all covalent-bonded interactions. Macchi and Sironi[12] have since observed that M atoms are always characterized by diffuse ns valence electrons, resulting

in a low local concentration of the electron density along the bond vectors for covalently bonded materials. As such, the Laplacian, the universal indicator of electron localization, can be close to zero and positive in sign in some cases, and it is considered to be an unsatisfactory tool for classifying bond type in general.[12] Earlier it was also observed by Cremer and Kraka[2] that intermediate-bonded interactions with Laplacian values falling within the range $2G(\mathbf{r}_c) > |V(\mathbf{r}_c)| > G(\mathbf{r}_c)$ of the local form of the virial equation are not covered by the Bader-Essén[10] classification scheme, and accordingly, they were classified as closed-shell ionic. Given this gap in the values of the local potential-energy density, Cremer and Kraka[2] proposed a classification scheme based solely on the local electronic energy density, $H(\mathbf{r}_c)=G(\mathbf{r}_c)+V(\mathbf{r}_c)$. Inasmuch as local kinetic-energy density is always positive and local potential-energy density is always negative, the sign of local electronic energy density necessarily determines whether the local potential-energy density or the local kinetic-energy dominates at $\mathbf{r}_c$. When the local potential-energy density is greater than the local kinetic-energy density, then a localization of electron density at $\mathbf{r}_c$ has a stabilizing impact on the system whereas when local kinetic-energy density is greater than the local potential-energy density, it has a destabilizing impact. On the basis of these relationships, Cremer and Kraka[2] classified a bonded interaction as either covalent when $|V(\mathbf{r}_c)| > G(\mathbf{r}_c)$ (the localization of electron density at $\mathbf{r}_c$ has a stabilizing impact on the system) or ionic when $G(\mathbf{r}_c) > |V(\mathbf{r}_c)|$ (the localization of electron density at $\mathbf{r}_c$ has a destabilizing impact on the system). On this basis, the double and triple C–O bonds classify as covalent[2] rather than ionic interactions with $H(\mathbf{r}_c)$ values of −1877 and −2150 kJ/mol/a_0^3, respectively, where a_0 is 1 bohr. Further, Li–O and Li–F bonded interactions, for example, with positive $H(\mathbf{r}_c)$ values of +48 and +63 kJ/mol/a_0^3 classify as ionic as expected from electronegativity considerations. However, the Cremer and Kraka[2] strategy is deficient in that it only serves to classify a bond as being either covalent or ionic; no criteria were given for classifying bonded interactions of intermediate type other than the case where $H(\mathbf{r}_c)=0$.

Hill *et al.*[13] have since evaluated the bond critical point and local electronic energy density values for a variety of hydroxyacid acid molecules involving first- and second-row *M* atoms and found, as may be expected, that the magnitude of local electronic energy density tends to increase with the electronegativity of the *M* atoms for a number of first- and second-row *M*–O bonded interactions. On the basis of their positive local electronic energy density values, the Li–O, Be–O, Na–O, Mg–O, and Al–O bonds are indicated to be predominately ionic in character whereas on the basis of their negative values, the B–O, C–O, N–O, Si–O, P–O, and S–O bonds are indicated to be predominately covalent in character. However, on the basis of their intermediate negative local electronic energy density values and their small $\rho(\mathbf{r}_c)$ values, the B–O and Si–O interactions were considered to be bonds of intermediate type. It was also found that the individual geometry-optimized *M*–O bond lengths for the molecules decrease nonlinearly as both $\rho(\mathbf{r}_c)$ and the Laplacian increase and as the χ value for the *M* atoms tend to increase from left to right in the periodic table. More recently, the bond critical point properties, calculated for a relatively large number of oxide earth materials, were found to show similar trends with the observed bond lengths.[14]

More recently, Espinosa *et al.*[15] calculated the bond critical point and the local energy density properties for isolated pairwise hydrogen fluoride H–F bonded interactions for 37 different *R*(H–F) bond lengths, ranging between 0.80Å and 2.50 Å, and found that the closed-shell bonded interactions for the dimers can be classified on the basis of the $|V(\mathbf{r}_c)|/G(\mathbf{r}_c)$ ratio as either shared covalent, closed-shell ionic, or as intermediate interactions. Bonded interactions exhibiting local electronic energy density values less than or equal to 0.0 with ratio values of less than 1.0 were classified as closed-shell ionic, while those exhibiting Laplacian values less than zero with ratio values greater than 2.0 were classified as covalent. The remaining bonded interactions with ratio values between 1.0 and 2.0 were classified as intermediate bonded interactions between ionic and covalent. In addition, 79 *X*-HF-*Y* neutral and positively and negatively charged complexes were theoretically considered and analyzed in terms of their bond critical point and energetic properties were also calculated at the complete active self-consistent-field (CASSCF) 6-311++G^{**} level. The bonded interactions for these complexes classify in terms of their $|V(\mathbf{r}_c)|/G(\mathbf{r}_c)$ ratios in virtually the same way as the HF dimers on the basis of their $H(\mathbf{r}_c)$ and $\nabla^2\rho(\mathbf{r}_c)$ values.

In a multipole modeling of the experimental electron-density distribution for the chain silicate diopside, $CaMgSi_2O_6$, Bianchi *et al.*[16] concluded, on the basis of the $|V(\mathbf{r}_c)|/G(\mathbf{r}_c)$ ratios (0.69-0.84), that the Ca–O and Mg–O bonds classify as purely ionic closed-shell interactions. On the other hand, as the ratios for the Si–O bonded interactions fall in the range between 1.13 and 1.38, they qualify as intermediate-type bonded interactions but with a substantial component of ionic character. As the average ratio for the longer Si–O bridging bonds of the pyroxene chain is smaller (~1.18) than that observed for the Si–O nonbridging bonds (~1.38), it was concluded that the longer bridging bonds (1.67 Å, on avcrage) are more ionic than the shorter nonbridging ones (1.59 Å, on average). They also observed that the ratios for the SiO bonds for the two silica polymorphs coesite (1.17) and stishovite (~1.19) are virtually the same. Given that coordination number of the Si atom in coesite is 4 with a SiO bond length is 1.61 Å, and that the coordination number of the atom is 6 in stishovite with a bond length of 1.76 Å, it is not evident why the $|V(\mathbf{r}_c)|/G(\mathbf{r}_c)$ ratios for the two polymorphs are nearly the same, particularly, given that the coordination number of Si in stishovite is larger than that in coesite and that the ratio for the longer bridging Si–O bonds in diopside is smaller than that for the shorter nonbridging bonds. The current study was undertaken to learn whether the three $|V(\mathbf{r}_c)|/G(\mathbf{r}_c)$ regions determined for the hydrogen fluorides provide a sound basis for classifying the *M*–O bond types for the oxide materials.

METHODOLOGY

The bond critical point properties for a large number of oxide crystals with first- and second-row *M*O bonded interactions were previously calculated,[14,17] using the programs CRYSTAL 98 (Ref. 18) and TOPOND.[19] The electronic structure for each crystal was calculated within the framework of reciprocal space using Bloch functions, expanded as linear combinations of atomic-centered Gaussian basis-set functions. Self-consistent-field wave functions were calculated for the experimental structures at the density-functional level of the theory using the Kohn-Sham[20] scheme. The local-density approximation was used as formulated by the local spin-density approximation by Dirac[21] for the exchange potential and the Vosko-Wilk-Nusair[22] parametrization of the correlation potential. All electron basis sets, specifically optimized for use in the CRYSTAL program,[18] were used. TOPOND (Ref. 19) was used to map the bond paths between bonded atoms to locate each nonequivalent $(3,-1)$ bond critical point and to calculate values for the electron density and the Hessian matrix at the points. The calculations show that as the values of $\rho(\mathbf{r}_c), \lambda_1, \lambda_2, \lambda_3$, and $\nabla^2\rho(\mathbf{r}_c)$ each increases in magnitude, the experimental *M*–O bonds decrease in length. In other words, as the bond decreases in length, the electron density is not only localized at $\mathbf{r}_c$, but also it is locally concentrated both perpendicular and parallel to the bond path at $\mathbf{r}_c$. The local concentration of ρ parallel to the bond path away from $\mathbf{r}_c$ serves to shield the nuclei of the bonded atoms.[14]

For this study, the local kinetic-energy density, the local potential-energy density, and the $|V(\mathbf{r}_c)|/G(\mathbf{r}_c)$ ratio were evaluated for each of the nonequivalent *M*–O bonded interactions for the oxide crystals with first- and second-row *M* atoms. In addition, as no earth materials to our knowledge possess C–O and N–O double and triple bonds, bond critical points and local energy density properties were calculated for CO, CO_2, H_2CO, H_3COH, H_4CO_4, H_6C_3O, NO, NO_2, H_2NO, H_2NOH, and H_3NO4 molecules, each geometry optimized and the electron density and bond critical point properties were generated at the B3LYP 6-311++$(3df,2p)$ level.

In this study, the connection will be examined between the values of the observed and calculated bond lengths, $R(M\text{–O})$, and the $\rho(\mathbf{r}_c), \nabla^2\rho(\mathbf{r}_c), G(\mathbf{r}_c), V(\mathbf{r}_c)$, and $H(\mathbf{r}_c)$ values calculated for the *M*–O bonded interactions for the oxides, for the C–O and N–O bond bearing molecules, and for the H–F bonded interaction for the HF dimers[14,15,17] to establish the extent to which they conform with the $|V(\mathbf{r}_c)|/G(\mathbf{r}_c)$ ratio classification of Espinosa *et al.*[15] It will be of interest to explore the extent to which the defining limits of 1.0 and 2.0 for ratios determined for the H–F dimers for zero values of $H(\mathbf{r}_c)$ and $\nabla^2\rho(\mathbf{r}_c)$, respectively, correspond with those determined for the oxides.

BOND LENGTH, CRITICAL POINT, AND LOCAL ENERGY DENSITY PROPERTIES: A COMPARISON

The electron-density values $\rho(\mathbf{r}_c)$ calculated for the *M*–O bonded interactions for the oxide materials with first- and second-row *M* metal atoms, (Li, Be, and B; Na, Mg, Al, Si, P, and S),[14] those for molecules with C–O and N–O bonded interactions and those for H–F bonded interactions (data taken from Table I of Espinosa *et al.*[15]) are plotted against the observed and calculated bond lengths, $R(M\text{–}X)$, in Fig. 1 (X=O,F). As the value of $\rho(\mathbf{r}_c)$ increases for each bonded interaction, the bond lengths decrease nonlinearly in a power-law trend. As such, the longer bonds show a greater decrease in length for a given increase in the value of $\rho(\mathbf{r}_c)$ than the shorter ones. In addition, the trends show little or no overlap with each bond type displaying a more or less singular power-law trend. The $\rho(\mathbf{r}_c)$ values for the H–F bonded interactions display a similar power-law trend but involve shorter bonds than those displayed by *M*–O bonded interactions.

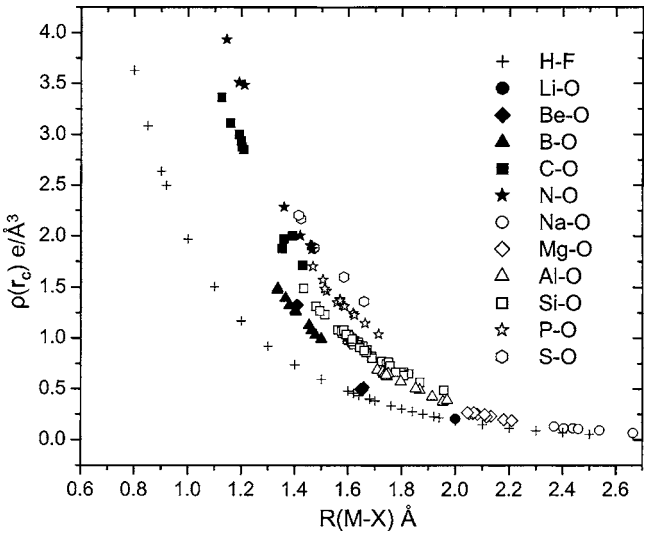

FIG. 1. Scatter diagrams (a) of the value of the electron density, $\rho(\mathbf{r}_c) \times (e/\text{Å}^3)$, evaluated at the $(3,-1)$ bond critical points $\mathbf{r}_c$ vs the bond lengths, $R(M\text{–}X)$(Å), for *M*–O bonded interactions (Ref. 14) involving first- and second-row *M* atoms bonded to O and H–F bonds for the HF dimer (Ref. 15).

The values of the local kinetic- and potential-energy densities generated for the oxide crystals, the molecules and the H–F dimers are plotted against $R(M\text{–}X)$ in Figs. 2(a) and 2(b), respectively. As observed for the H–F dimers, the magnitude of $V(\mathbf{r}_c)$ increases at a faster rate for the oxides with decreasing bond length than $G(\mathbf{r}_c)$, indicating that the materials are progressively stabilized with decreasing bond length and increasing $\rho(\mathbf{r}_c)$. Likewise, the $G(\mathbf{r}_c)$ values for the C–O and N–O bonds tend to increase at a faster rate with decreasing bond length than the remaining first-row and second-row *M*–O bonds. These relationships are borne out by Fig. 3(a) where the $H(\mathbf{r}_c)=G(\mathbf{r}_c)+V(\mathbf{r}_c)$ values are plotted against $R(MX)$. The more ionic Li–O, Be–O, Na–O, Mg–O, Al–O, and Si–O bonded interactions tend to closely follow the HF dimer trend of the $H(\mathbf{r}_c)$ versus $R(M\text{–}X)$ in the range between 1.45 Å and 2.65 Å whereas the values for the more covalent B–O, C–O, N–O, P–O, and S–O bond lengths tend to parallel the dimer trend but displaced to longer bond lengths. The local potential-energy density is highly correlated with bond length and decreases rapidly with decreasing bond length for the more electronegative *M* atoms. On the basis of the Cremer and Kraka[2] criteria, the Li–O, Na–O, and

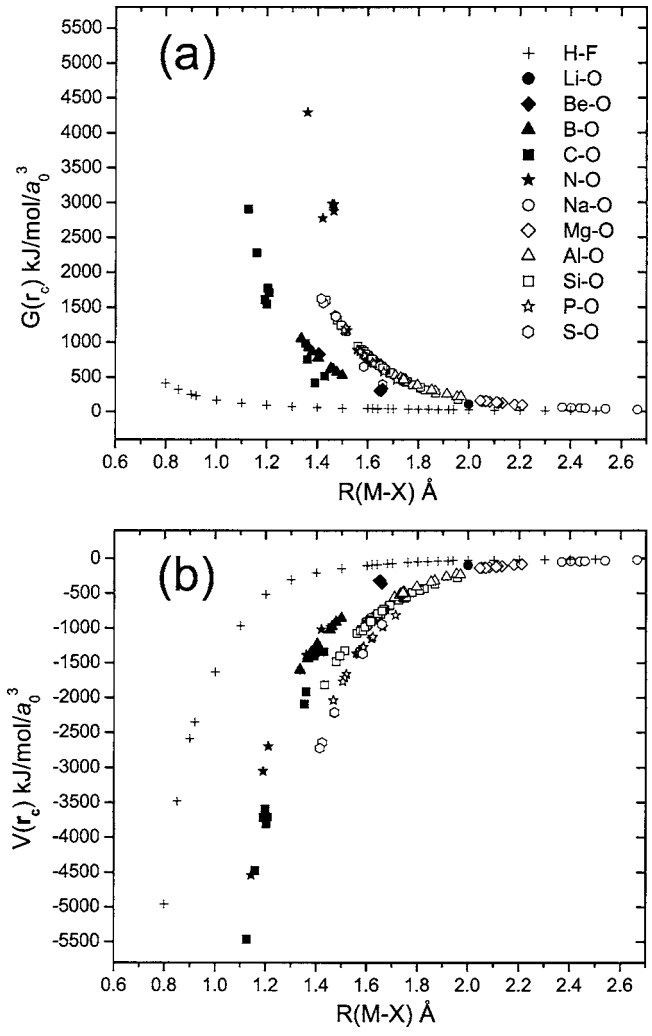

FIG. 2. (a) $G(\mathbf{r}_c)$, the local kinetic-energy density (kJ/mol/a_0^3) evaluated at $\mathbf{r}_c$ vs $R(M–X)$(Å) and (b) $V(\mathbf{r}_c)$, the local potential-energy density (kJ/mol/a_0^3) evaluated at $\mathbf{r}_c$ vs $R(M–X)$(Å).

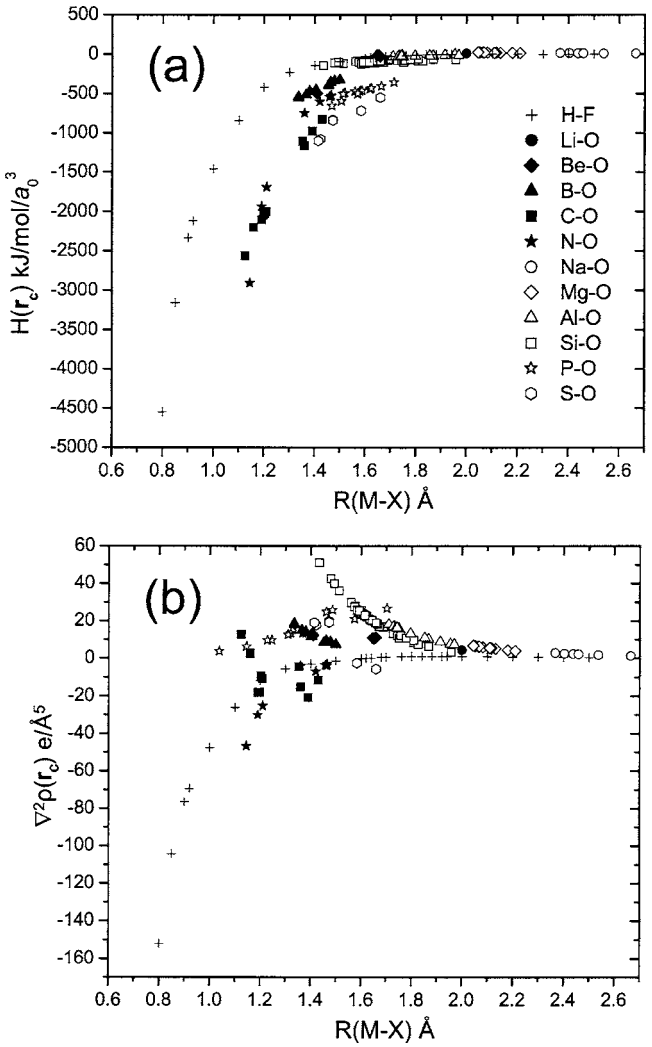

FIG. 3. (a) $H(\mathbf{r}_c)=G(\mathbf{r}_c)+V(\mathbf{r}_c)$, the local electronic density energy (kJ/mol/a_0^3) evaluated at $\mathbf{r}_c$ vs $R(M–X)$(Å) and (b) $\nabla^2\rho(\mathbf{r}_c)$, the Laplacian of $\rho(\mathbf{r}_c)$(e/Å^5) evaluated at $\mathbf{r}_c$ vs $R(M–X)$(Å).

Mg–O bonded interactions with positive $H(\mathbf{r}_c)$ values qualify as closed-shell ionic bonds whereas the remaining $M–X$ bonds with negative $H(\mathbf{r}_c)$ values qualify as covalent bonds.

Figure 3(b) displays the trends between $\nabla^2\rho(\mathbf{r}_c)$ and $R(M–X)$. The value of the Laplacian increases slightly for the HF dimer from a value of 0.5 e/Å^5 for a bond length of 2.50 Å to a maximum at 1.14 e/Å^5 at 1.90 Å. It then decreases with decreasing bond length, becoming negative at 1.60 Å and adopts a value of −150 e/Å^5 at a bond length of 0.80 Å.[15] The Laplacian values for a number of the first- and second-row M–O bonded interactions (B–O, C–O, Mg–O, Al–O, Si–O, and S–O) each increases with decreasing bond length. In contrast, the values for the P–O and N–O bonds decrease with the $\nabla^2\rho(\mathbf{r}_c)$ values for the N–O bonds displaying negative values and those for the P–O bonds displaying positive values. According to the Bader and Essén[10] criteria based on the values of $\nabla^2\rho(\mathbf{r}_c)$, the Li–O, Be–O, B–O, Na–O, Mg–O, Al–O, Si–O, and P–O bonded interactions each qualify as closed-shell ionic interactions while the N–O and several of the C–O and S–O bonded interactions qualify as shared covalent interactions.

Scatter diagrams of the $|V(\mathbf{r}_c)|/G(\mathbf{r}_c)$ ratio versus $H(\mathbf{r}_c)$ and $\nabla^2\rho(\mathbf{r}_c)$, respectively, for the HF dimer determined by Espinosa *et al.*,[15] show that when $H(\mathbf{r}_c)\approx 0$, the ratio ≈ 1.0 and that when $\nabla^2\rho(\mathbf{r}_c)\approx 0.0$, then the ratio ≈ 2.0. When the value of $H(\mathbf{r}_c)$ is positive, a bonded interaction is considered by Cremer and Kraka[2] to be closed-shell ionic and when the value of $\nabla^2\rho(\mathbf{r}_c)$ is negative, a bonded interaction is considered by Bader and Essen[10] to be shared covalent. Accordingly, when the value of the ratio is 1.0 or smaller, the local electronic energy density is necessarily positive and the bonded interaction is defined as closed-shell ionic. On the other hand, when the value of the ratio is 2.0 or greater, the Laplacian is necessarily negative and the bonded interaction is defined as shared covalent. Finally, the bonded interactions with ratio values between 1.0 and 2.0 are defined as intermediate interactions.[15]

The ratio values for the HF dimers and the oxides are plotted against the local electronic energy density and the Laplacian in Figs. 4(a) and 4(b), respectively. With increasing ratio, the local electronic energy density and the Laplacian values for the dimers both increase slightly above zero and then decrease and become negative. The $H(\mathbf{r}_c)$ versus $|V(\mathbf{r}_c)|/G(\mathbf{r}_c)$ trend crosses at $H(\mathbf{r}_c)\approx 0$ and $|V(\mathbf{r}_c)|/G(\mathbf{r}_c)$

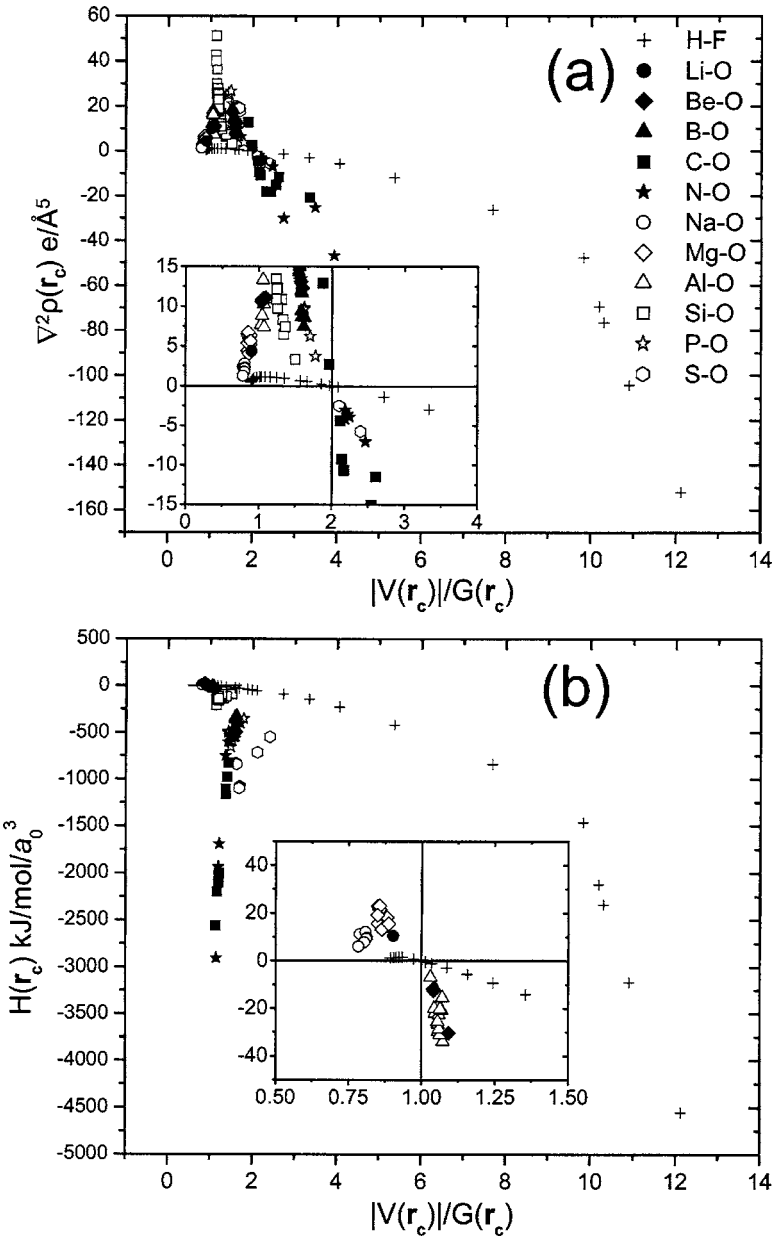

FIG. 4. (a) Scatter diagrams of $\nabla^2\rho(\mathbf{r}_c)(e/\text{Å}^5)$, the Laplacian of $\rho(\mathbf{r}_c)$ evaluated at $\mathbf{r}_c$ vs the $|V(\mathbf{r}_c)|/G(\mathbf{r}_c)$ ratio and (b) $H(\mathbf{r}_c)=G(\mathbf{r}_c)+V(\mathbf{r}_c)$ vs the $|V(\mathbf{r}_c)|/G(\mathbf{r}_c)$ ratio for M–O bonded interactions involving first- and second-row M atoms bonded to O, and H–F bonds for the HF dimer (Ref. 15). The inserts provided a magnified view of the scatter diagrams where $\nabla^2\rho(\mathbf{r}_c)$ and $H(\mathbf{r}_c)$ both adopt a value of zero. The data cross the $\nabla^2\rho(\mathbf{r}_c)=0$ line at a $|V(\mathbf{r}_c)|/G(\mathbf{r}_c)$ value of ~2 and the $H(\mathbf{r}_c)=0$ line at a $|V(\mathbf{r}_c)|/G(\mathbf{r}_c)$ value of ~1.

≈ 1 while the $\nabla^2\rho(\mathbf{r}_c)$ versus $|V(\mathbf{r}_c)|/G(\mathbf{r}_c)$ trend crosses at $\nabla^2\rho(\mathbf{r}_c)\approx 0$ and $|V(\mathbf{r}_c)|/G(\mathbf{r}_c)\approx 2$ in apparent agreement with the arguments of Espinosa *et al.*[15] As displayed in Figs. 2(a) and 2(b), the trends between local potential-energy density and local kinetic-energy density versus $R(M–X)$ are substantially different for the H–F and M–O bonded interactions. Given these differences, it might be expected that the coordinates of the crossing point for $|V(\mathbf{r}_c)|/G(\mathbf{r}_c)$ with $\nabla^2\rho(\mathbf{r}_c)$ and $H(\mathbf{r}_c)$ should depart significantly from (2,0) and (1,0), respectively, for the M–O bonded interactions. But a careful examination of the inserts in the two figures [Figs. 4(a) and 4(b)] shows that the $\nabla^2\rho(\mathbf{r}_c)$ and $H(\mathbf{r}_c)$ trends for the oxide data intersect $|V(\mathbf{r}_c)|/G(\mathbf{r}_c)$ at nearly the same points as observed for the HF dimers. In other words, it appears that the three $|V(\mathbf{r}_c)|/G(\mathbf{r}_c)$ regions defined for classifying the nature of a bond are universal in their application, at least to the extent that holds for M–O bonded interactions. According to Espinosa *et al.*,[15] closed-shell ionic interactions display $|V(\mathbf{r}_c)|/G(\mathbf{r}_c)$ ratio values less than 1.0 (region I) $[H(\mathbf{r}_c)>0]$, intermediate interactions $1<|V(\mathbf{r}_c)|/G(\mathbf{r}_c)<2[-G(\mathbf{r}_c)<H(\mathbf{r}_c)<0]$ (region II), and covalent interactions $|V(\mathbf{r}_c)|/G(\mathbf{r}_c)>2[H(\mathbf{r}_c)<-G(\mathbf{r}_c)]$ (region III).

On the basis of their ratios, Na–O (0.70–0.76), Li–O (0.84), and Mg–O (0.85–0.89) qualify as closed-shell ionic bonds, Be–O (0.99-1.54), Al–O (1.05-1.07), Si–O (1.12-1.34), B–O (1.50-1.55), and P–O (1.41-1.78) each qualify as bonds of intermediate character, and N–O (2.19-3.93) qualifies as shared covalent. The C–O and S–O bonds with ratios between 1.88 and 3.35 and 1.61 and 2.40, respectively, qualify as both intermediate and covalent bonds. The C–O triple bond, with a ratio of 1.87, is classified as a bond of intermediate character whereas according to its $H(\mathbf{r}_c)$ value (-2557.8 kJ/mol/a_0^3), it classifies as covalent and according to its Laplacian value (12.88 $e/\text{Å}^5$), it classifies as an ionic bond. The decrease in the ratio for the C–O bond from 3.35 for a single bond to 2.03 for a double bond to 1.88 for a triple bond can be related to the increase in the spectroscopically based electronegativities[4] of the C atoms associated

with the increase in the *s* character of the atom coupled with a concomitant increase in the ionic character of the bond.[4] The ratios for the Be–O, Al–O, and Si–O bonds indicate that these bonds have a substantial component of ionic bonding despite their classification as bonds of intermediate character. The trend between the ratio and the character of the bonded interaction is consistent with trends expected from electronegativity considerations.

It is expected that the larger the value of the ratio for a given bonded interaction falling in region II, the more covalent the bonded interaction. For example, the covalent character of the B–O bond with ratio values between 1.50-1.55 is indicated to be greater than that of the Si–O bond with ratio values ranging between 1.12-1.34. Accordingly, the SiO bond in stishovite with six-coordinate Si and a Si–O bond length of 1.783 Å and a ratio of 1.19 is indicated to be slightly more covalent than the Si–O bonds in forsterite, Mg_2SiO_4, with four-coordinate Si, a Si–O bond length of 1.635 Å and with a ratio 1.16. This result is at variance with the studies of Mooser and Pearson,[6] that indicate that the bonding in six-coordinated polyhedra comprising MX_2 materials is usually more ionic than that in materials with four-coordinated polyhedra. It is also at variance with the experimentally determined net atomic charges for the Si atoms comprising the SiO_4 tetrahedra in forsterite[23] and those comprising the SiO_6 octahedra in stishovite.[24] By integrating the experimental model multipole electron-density distributions over the range of the atomic basins[25] for the two Si atoms, the net charge conferred on the Si atom in forsterite, $Q(\mathrm{Si}) = +3.17e$, was found to be less than that determined for the Si atom in stishovite, $Q(\mathrm{Si}) = +3.39e$, indicating, on the contrary, that the SiO bond in stishovite is slightly more ionic than that in forsterite. Further, a recent study of several Ni sulfides revealed that the net charge on the Ni atom increases from $+0.31e$ to $+0.52e$ as the NiS bond increases in length from 2.27 to 2.40 Å and the coordination number of the Ni atom increases from four to six,[26] and the ratio decreased from 1.26 to 1.20. In this case, the ratio indicates, unlike the case for the SiO bond, that the ionic character of the NiS bond increases as the coordination number of the Ni atom increases. In short, it is evident that the ratio for a bonded interaction in a given region of ratios does not always reflect a change in bond character that is consistent with the connection established earlier by Phillips[1] between ionicity and coordination number and the connection between coordination number and the net atomic charges.

The presence of well-developed domains of localized electron density along the bond vectors and in the nonbonded regions of a material are features that are generally associated with covalent bonded interactions. Despite the substantial ionic component of the Si–O bond indicated by their $|V(\mathbf{r}_c)|/G(\mathbf{r}_c)$ ratios, diopside,[16] forsterite,[23] coesite,[27] and stishovite[24] each display well-developed domains of experimental and theoretical model electron densities along the Si–O bond vectors. Each of these earth materials also displays well-developed domains in the nonbonded regions of the O atoms, suggesting that the bond is intermediate in character with a substantial component of covalent character.

CONCLUSIONS

Our study of the bond critical point and the local energy properties for oxide molecules and earth materials yielded three $|V(\mathbf{r}_c)|/G(\mathbf{r}_c)$ bond-type regions that agree in large part with those determined for H–F bonded interactions. The agreement demonstrates that the strategy of Espinosa *et al.*[15] is universal to the extent that it also holds for M–O bonded interactions in molecules and earth materials. However, the trend between the ratio and the coordination number for silicates with four- and six-coordinate Si is at variance with the trends established between the coordination number and bond type.[1,6] Albeit that the strategy does a reasonably good job classifying bonded interactions for oxides and fluorides, additional studies are needed, for example, for chalcogenides, pnictides, intermetallic compounds, metals, and related materials, to establish, on the one hand, the universality of the classification,[15] and to improve, on the other hand, our understanding of the connection between the ratio, the coordination number, the bond length, and the net atomic charges of the bonded atoms. A recent calculation[26] of the $|V(\mathbf{r}_c)|/G(\mathbf{r}_c)$ ratio for the Ni–Ni bonded interactions comprising bulk Ni metal yielded a value of 1.28, a result that indicates, according to the arguments of Espinosa *et al.*[15] that the bonded interactions in the metal are intermediate with a substantial component of ionic character. Finally, it is evident that the ratio for a bonded interaction may not always reflect the change in bond character as expected from an increase in the net atomic charge and coordination number of the Si atom.

ACKNOWLEDGMENTS

The National Science Foundation and the U.S. Department of Energy are thanked for supporting this study in part with Grant Nos.EAR-0229472 (N.L.R. and G.V.G.), DE-FG02-03ER15389 (JD Rimstidt, G.V.G.), and DE-FG02-97ER14751 (D.F.C.). This research was done in part using the Molecular Science Computing Facility (MSCF) in the William R. Wiley Environmental Molecular Sciences Laboratory, a national scientific user facility sponsored by the U.S. Department of Energy's Office of Biological and Environmental Research and located at the Pacific Northwest National Laboratory. Pacific Northwest is operated for the Department of Energy by Battelle. One of the authors (G.V.G.) wishes to thank Professor Bianchi of the CNR Institute of Science and Technology at Milano Italy for bringing to his attention Professor Espinosa's paper on the $|V(\mathbf{r}_c)|/G(\mathbf{r}_c)$ ratio, its use in classifying H–F bonded interactions and, in particular, his paper on diopside that stimulated a good discussion, despite G.V.G.'s doubts about the universality of the ratio in classifying bonded interactions.

[1] J. C. Phillips, Rev. Mod. Phys. **42**, 317 (1970).
[2] D. Cremer and E. Kraka, Croat. Chem. Acta **57**, 1259 (1984).
[3] L. Pauling, *The Nature of the Chemical Bond* (Cornell University Press, Ithaca, NY, 1939).
[4] L. C. Allen, J. Am. Chem. Soc. **111**, 9003 (1989).
[5] J. C. Phillips, in *Treatise on Solid State Chemistry*, edited by N. B. Hannay (Plenum, New York, 1974), p. 1.
[6] E. Mooser and W. B. Pearson, Acta Crystallogr. **12**, 1015 (1959).
[7] A. Zunger, in *Structure and Bonding in Crystals*, edited by M. O'Keeffe

and A. Navrotsky (Academic, New York, 1981), Vol. 1, p. 73.
[8] A. N. Bloch and G. C. Schatteman, in *Structure and Bonding in Crystals*, edited by M. O'Keeffe and A. Navrotsky (Academic, New York, 1981), Vol. 1, p. 49.
[9] R. F. W. Bader, *Atoms in Molecules* (Oxford Science, Oxford, UK, 1990).
[10] R. F. W. Bader and H. Essén, J. Chem. Phys. **80**, 1943 (1984).
[11] G. V. Gibbs, D. F. Cox, K. M. Rosso, A. Kirfel, T. Lippmann, P. Blaha, and K. Schwarz, Phys. Chem. Miner. **32**, 114 (2005).
[12] P. Macchi and A. Sironi, Coord. Chem. Rev. **238**, 383 (2003).
[13] F. C. Hill, G. V. Gibbs, and M. B. Boisen Jr., Phys. Chem. Miner. **24**, 582 (1997).
[14] G. V. Gibbs, M. B. Boisen, L. L. Beverly, and K. M. Rosso, in *Molecular Modeling Theory: Applications in the Geosciences*, edited by J. D. Kubicki (Mineralogical Society of America, Washington, DC, 2001), Vol. 42, p. 345.
[15] E. Espinosa, I. Alkorta, J. Elguero, and E. Molins, J. Chem. Phys. **117**, 5529 (2002).
[16] R. Bianchi, A. Forni, and R. Oberti, Phys. Chem. Miner. **32**, 638 (2005).
[17] R. T. Downs, G. V. Gibbs, M. B. Boisen, Jr, and K. M. Rosso, Phys. Chem. Miner. **29**, 369 (2002).
[18] V. R. Saunders, R. Dovesi, C. Roetti, M. Causa, N. M. Harrison, R. Orlando, and E. Apra, *CRYSTAL 98 User's Manual* (University of Torino, Torino, Italy, 1998).
[19] C. Gatti, *TOPOND 96 User's Manual* (CNR-CSRSRC, Milano, Italy, 1997).
[20] W. Kohn and L. J. Sham, Phys. Rev. **140**, A1133 (1965).
[21] P. A. M. Dirac, *The Principles of Quantum Mechanics* (Oxford University Press, Oxford, UK, 1958).
[22] S. H. Vosko, L. Wilk, and M. Nusair, Can. J. Phys. **58**, 1200 (1980).
[23] A. Kirfel, T. Lippmann, P. Blaha, K. Schwarz, D. F. Cox, K. M. Rosso, and G. V. Gibbs, Phys. Chem. Miner. **32**, 301 (2005).
[24] A. Kirfel, H. G. Krane, P. Blaha, K. Schwarz, and T. Lippmann, Acta Crystallogr., Sect. A: Found. Crystallogr. **A57**, 663 (2001).
[25] T. A. Keith, Ph.D. thesis, McMaster University, 1993.
[26] G. V. Gibbs, R. T. Downs, C. T. Prewitt, K. M. Rosso, N. L. Ross, and D. F. Cox, J. Phys. Chem. B **109**, 21788 (2005).
[27] G. V. Gibbs, A. E. Whitten, M. A. Spackman, M. Stimpfl, R. T. Downs, and M. D. Carducci, J. Phys. Chem. B **107**, 12996 (2003).